Eur. J. Mineral.
2015, **27**, 137–143
Published online 4 December 2014

Mayenite supergroup, part IV: Crystal structure and Raman investigation of Al-free eltyubyuite from the Shadil-Khokh volcano, Kel' Plateau, Southern Ossetia, Russia

FRANK GFELLER[1,*], DOROTA ŚRODEK[2], JOACHIM KUSZ[3,4], MATEUSZ DULSKI[3,4], VIKTOR GAZEEV[5], IRINA GALUSKINA[2], EVGENY GALUSKIN[2] and THOMAS ARMBRUSTER[1]

[1] Mineralogical Crystallography, Institute of Geological Sciences, University of Bern, Freiestrasse 3, 3012 Bern, Switzerland
*Corresponding author, e-mail: frank.gfeller@krist.unibe.ch
[2] Department of Geochemistry, Mineralogy and Petrography, Faculty of Earth Sciences, University of Silesia, Będzińska 60, 41–200 Sosnowiec, Poland
[3] Institute of Physics, University of Silesia, Uniwersytecka 4, 40–007 Katowice, Poland
[4] Silesian Center for Education and Interdisciplinary Research, 75 Pułku Piechoty 1a, 41–500 Chorzow, Poland
[5] Institute of Geology of Ore Deposits, Petrography, Mineralogy and Geochemistry (IGEM) RAS, Staromonetny 35, Moscow, Russia

Abstract: Eltyubyuite, ideally $Ca_{12}Fe^{3+}{}_{10}Si_4O_{32}Cl_6$, a member of the mayenite supergroup, was originally described from altered xenoliths of the Upper Chegem, northern Caucasus, Russia, and Eifel, Germany, where it forms a solid-solution with wadalite ($Ca_{12}Al_{10}Si_4O_{32}Cl_6$). The structure of the holotype was confirmed earlier using electron backscatter diffraction. The larger crystal size of Al-free eltyubyuite from a new occurrence in an altered carbonate–silicate xenolith enclosed in plagiodacites of the Shadil-Khokh volcano, Kel' Plateau, Southern Ossetia, enabled the first direct refinement of the eltyubyuite crystal structure. At this locality, Al-free eltyubyuite occurs in a contact zone of the xenolith, within small veins composed of rusinovite, cuspidine and rondorfite. The structure of the Al-free eltyubyuite crystal (dimensions: 20 × 15 × 10 μm) was refined from X-ray diffraction data to $R_1 = 0.019$. Eltyubyite (cubic, space group $I\bar{4}3d$, $a = 12.2150$ (2) Å, $V = 1822.55(6)$ Å^3, $Z = 2$) is isostructural with mayenite. Both tetrahedra are Fe^{3+}-dominant: the $T1$ site (= 1.848 Å) contains 0.85 Fe^{3+} and 0.15 Si^{4+}, whereas the $T2$ site (= 1.766 Å) has 0.59 Fe^{3+} and 0.41 Si^{4+}. Based on electron microprobe data, the empirical formula of eltyubyuite from Ossetia is $Ca_{12.044}(Fe^{3+}{}_{10.373}Si_{3.473}Ti^{4+}{}_{0.067}Mn^{2+}{}_{0.021}Mg_{0.021})_{\sum 13.956}O_{32}Cl_{5.455}$. Raman spectroscopy recorded bands with increased half-width due to Fe^{3+} and Si^{4+} disorder at the two tetrahedral sites $T1$ and $T2$. The Raman bands at 959 and 901 cm^{-1} have been assigned to Si–O stretching vibrations (ν_1 and ν_3) of $(SiO_4)^{4-}$. The group of bands at 783 (ν_3), 705 (ν_1), 450 (ν_4), 307 (ν_2) cm^{-1} correspond to Fe–O vibration of $(Fe^{3+}O_4)^{5-}$.

Key-words: Eltyubyuite; wadalite; mayenite supergroup; crystal structure; Raman spectroscopy; Shadil-Khokh volcano; Southern Ossetia.

Introduction

Eltyubyuite, ideally $Ca_{12}Fe^{3+}{}_{10}Si_4O_{32}[Cl_6]$, was first described from altered carbonate–silicate xenotliths enclosed in ignimbrites of the Upper Chegem caldera in Kabardino-Balkaria, northern Caucasus, Russia. The holotype empirical formula was $Ca_{12.12}Mg_{0.04}Ti_{0.11}Fe_{9.41}Al_{1.26}Si_{2.98}O_{31.89}Cl_{5.04}$ and, due to the very small crystal size (Galuskin *et al.*, 2013), its structure was determined using electron backscatter diffraction (EBSD).

Eltyubyuite is the Fe end-member of the wadalite-group, a subdivision of the mayenite supergroup (Galuskin *et al.*, 2015a). The wadalite group is represented by silicates isostructural with mayenite, $Ca_{12}Al_{14}O_{32}[O]$, and comprises the mineral species wadalite, $Ca_{12}Al_{10}Si_4O_{32}[Cl_6]$ (Tsukimura *et al.*, 1993), and eltyubyuite, $Ca_{12}Fe^{3+}{}_{10}Si_4O_{32}[Cl_6]$ (Galuskin *et al.*, 2013). The crystal structure of compounds belonging to the mayenite supergroup is based on a tetrahedral framework $\{T_{14}O_{32}\}$ that encloses six structural cages per formula unit (pfu) (Büssem & Eitel, 1936). Depending on the type of tetrahedrally coordinated cations in the framework (Mg^{2+}, Al^{3+}, Fe^{3+}, Si^{4+} Ti^{4+}), the negative framework charge ranges between –18 and –22. Each of the structural cages is occupied by two Ca^{2+} (charge +24 pfu), which results in an excess positive charge ranging between +2 (mayenite group) and +6 (wadalite group). The charge is balanced by anions at the central [W] site of the structural cages. The

DOI: 10.1127/ejm/2015/0027-2421
0935-1221/15/0027-2421 $ 3.15

general formula $X_{12}T_{14}O_{32}[W]_6$ has been introduced for minerals of the mayenite supergroup, and end-members of the wadalite group are characterized by a charge sum at the *W* sites of –6 pfu (Galuskin *et al.*, 2015a).

Wadalite-group minerals have been reported from six terrestrial occurrences: (1) wadalite enclosed in a two-pyroxene andesite in Tadona near Koriyama City, Fukushima Prefecture, Japan (Tsukimura *et al.*, 1993), (2) wadalite from the La Negra mine, Queretaro, Mexico (Kanazawa *et al.*, 1997), (3) wadalite from the Wiluy River, Sakha (Yakutia), Russia (Galuskin *et al.*, 2007), (4) Fe-rich wadalite from the Bellerberg Volcano, Eifel, Germany (Mihajlović *et al.*, 2004), (5) wadalite and eltyubyuite from the Upper Chegem caldera (Galuskin *et al.*, 2013), and (6) wadalite and eltyubyuite from the Shadil-Khokh volcano, Southern Ossetia (Galuskin *et al.*, 2013: this study).

In addition, wadalite has been found in Ca-Al-rich inclusions (CAI) of several meteorites, for example igneous type-B CAI from the CV carbonaceous chondrite Allende (Ishii *et al.*, 2010). In meteorites, minerals of the wadalite group are hosts for Cl, whose isotopes are used to constrain the timing of the early solar system events (*e.g.*, Matzel *et al.*, 2010; Bowers *et al.*, 2013; Bricker & Caffee, 2013).

Beside natural occurrences, members of the wadalite group are found in combustion dumps: *e.g.*, in the Ca-rich metacarbonate rocks of the Donetsk Coal Basin (Sharygin, 2010) and in the Rosice-Oslavany coalfield, Czech Republic (Hršelová *et al.*, 2013).

Compounds isostructural with mayenite $Ca_{12}Al_{14}O_{32}[O]$ are exhaustively discussed in material science for their use as semiconductors or catalysts (*e.g.* Palacios *et al.*, 2007, 2008; Lee *et al.*, 2009; Sakakura *et al.*, 2011). The main reason for the high interest in the mayenite-type compounds is their microporosity and anion exchange capacity combined with high-temperature stability. The microporosity results from the partial occupation of the [*W*] site (Büssem & Eitel, 1936). In contrast to mayenite, the [*W*] site in wadalite-group compounds is almost completely occupied by Cl and therefore the ion-exchange capacity is strongly reduced. Moreover, silicates with mayenite-type structure are of interest to other branches of science and technology. Wadalite-like compounds are discussed as potential solids to immobilize elements from Cl-rich media: the immobilization of fission products from spent nuclear fuel after reprocessing in a chloride melt (Leturcq *et al.*, 2005; Park *et al.*, 2008). Another example is wadalite formation during the removal of HCl from effluent gases at high temperature (> 400°C) by a reaction with hydrogrossular (Fujita *et al.*, 2001, 2003).

Beside their role as host for waste elements, wadalite-like compounds are patented as mineral additive in, *e.g.*, the running surface of skis and snowboards (Cebocli *et al.*, 2007), electrode for a discharge lamp (*e.g.*, Ito *et al.*, 2012; Watanabe *et al.*, 2012) or as ceramic used in manufacturing of plasma displays (Ito & Webster, 2007).

Hitherto it was not possible to refine the crystal structure of eltyubyuite. The separation of a single crystal was not possible, since eltyubyuite tends to form thin overgrowths on other minerals of the mayenite supergroup (chlormayenite, wadalite, Galuskin *et al.*, 2013). However, we succeeded in separating a suitable grain from a sample from the Shadil-Khokh volcano, Kel' Plateau, Southern Ossetia, and thus we report here the first single-crystal X-ray diffraction (XRD) structure refinement and Raman spectroscopic characterization of Al-free eltyubyuite.

Occurrence

Eltyubeyuite was found in an altered carbonate–silicate xenolith (> 2 m in diameter) enclosed in dacite lavas on the north-west slope of the Shadil-Khokh volcano (age ~ 30 ka), Kel' volcanic area, Greater Caucasus Mountain Range, Southern Ossetia. The xenolith is composed of minerals that are characteristic of pyrometamorphic rocks (sanidinite facies), *i.e.* spurrite, larnite, gehlenite, merwinite, bredigite, rondorfite, and srebrodolskite (Gazeev *et al.*, 2012).

Eltyubyuite occurs in small veins up to 0.5 cm wide at the contact zone of the xenolith. The veins are mainly composed of rusinovite $Ca_{10}(Si_2O_7)_3Cl_2$ (second occurrence worldwide), cuspidine, $Ca_4(Si_2O_7)F_2$, and rondorfite, $MgCa_8(SiO_4)_4Cl_2$; rare crystals of eltyubyuite were found in small vugs filled by hydrocalumite (Table 1, Fig. 1). The adjacent altered xenolith appears as a bleached rock composed of low-temperature secondary minerals (70–80 vol.%) such as jennite, tobermorite-like minerals, and other unidentified Ca-hydrosilicates, hydrocalumite, ettringite-group minerals, grossular–katoite series minerals, and calcite. Moreover, relics of high-temperature Ca-silicate minerals such as larnite, merwinite, gehlenite, wollastonite, cuspidine, wadalite, magnesioferrite, Ti-bearing andradite were identified. Wollastonite, åkermanite, merwinite, monticellite, zoned aggregates of wadalite, eltyubyuite, rondorfite, and rusinovite were found in intimate contact with the volcanic rock.

The eltyubyuite crystals (Fig. 1B) are rare and their size does not usually exceed 20 μm; they typically feature tristetrahedral faces {211}.

Eltyubyuite is a characteristic constituent of Cl-bearing mineral associations formed in altered carbonate xenoliths within volcanic rocks as a result of complex metasomatism at high temperature and low pressure. During the metasomatic alteration of the sedimentary protolith, volcanic gases transported volatile components leading to the formation of new phases. In the case of Cl-rich fluids, rusinovite $Ca_{10}(Si_2O_7)_3Cl_2$ formed instead of rankinite $Ca_3Si_2O_7$, rondorfite $MgCa_8(SiO_4)_4Cl_2$ instead of bredigite $MgCa_7(SiO_4)_4$, and minerals of the mayenite supergroup instead of garnets (andradite–grossular series), gehlenite or ferrite-aluminates of the brownmillerite–srebrodolskite series.

Experimental procedure

Composition, Raman spectrum and crystal structure were determined on the largest crystal shown in Fig. 1B. An eltyubyuite grain $20 \times 15 \times 10$ μm in size was separated for the single-crystal XRD study.

Table 1. Experimental details for XRD data.

Crystal data	
Unit-cell dimensions (Å)	$a = 12.2150(2)$
Space group	$I\bar{4}3d$ (No. 220)
Volume (Å^3)	1822.55(6)
Z	2
Chemical formula	$Ca_{12}Fe_{10.33}Si_{3.67}O_{32}[Cl_{5.45}\square_{0.55}]$
Absorption coefficient μ cm^{-1}	52.766
Intensity measurement	
Crystal size (mm)	0.01 × 0.01 × 0.01
Diffractometer	SuperNova Dual diffractometer
X-ray radiation	Cu $K\alpha$
X-ray power	40 W
Monochromator	mirror
Temperature	100.0(1) K
Detector to sample distance	55 mm
Measurement method	ω-scans
Radiation width	SuperNova (Cu) micro X-ray source
Time per frame	120 sec
Max. 2θ°-range for data collection	64.28
Index ranges	$-13 \le h \le 13$ $-15 \le k \le 14$ $-15 \le l \le 13$
No. of measured reflections	4645
No. of unique reflections	312
No. of observed reflections ($I > 2\sigma$ (I))	300
Refinement of the structure	
No. of parameters used in refinement	39
R_{int}	0.0474
R_σ	0.0175
R_1, $I > 2\sigma(I)$	0.0190
R_1 all data	0.0206
wR_2 on (F^2)	0.0464
GooF	1.128
$\Delta\rho_{min}$ (-e Å^{-3})	−0.33 close to Si1
$\Delta\rho_{max}$ (e Å^{-3})	0.33 close to O1

The crystal morphology and chemical composition of eltyubyuite and associated minerals were examined using optical microscopes, an environmental scanning electron microscope (Philips XL30 ESEM/EDAX; Faculty of Earth Sciences, University of Silesia), and an electron microprobe (CAMECA SX100; Institute of Geochemistry, Mineralogy and Petrology, University of Warsaw). Electron microprobe (EMP) analyses of eltyubyuite were performed at 15 kV and 20 nA, *ca.* 1 μm beam diameter using the following lines and standards: Ca$K\alpha$, Si$K\alpha$ – wollastonite; Al$K\alpha$ – orthoclase, Cl$K\alpha$ – tugtupite; Fe$K\alpha$ – Fe_2O_3; Mn$K\alpha$ – rhodochrosite; Ti$K\alpha$ – rutile; Mg$K\alpha$ – diopside; Na$K\alpha$ – albite; F$K\alpha$, P$K\alpha$ – apatite BB2; S$K\alpha$ – barite.

Single-crystal XRD studies of eltyubyuite were carried out using a SuperNova Dual diffractometer with a mirror monochromator (Cu$K\alpha$, λ = 1.54184 Å) and Atlas CCD detector (Aligent Technologies) at the Institute of Physics, University of Silesia, Poland. The experiment was performed at 100 K. The data were processed using the software package of CrysAlisPro, Agilent Technologies. An empirical absorption correction using spherical harmonics, implemented in the SCALE3 ABSPACK scaling algorithm, was conducted. The structure was solved by direct methods, with subsequent analyses of difference-Fourier maps, and refined with neutral atom scattering factors using SHELXL (Sheldrick, 2008). Details for the single-crystal XRD measurement and the refinement are listed in Table 1.

The Raman spectra of eltyubyuite were recorded on a WITec confocal Raman microscope CRM alpha 300 equipped with an air-cooled solid-state laser, emitting at 532 nm, and a CCD camera operating at −58°C at the Institute of Physics, University of Silesia, Poland The excitation laser radiation was coupled into a microscope through a single-mode optical fibre with a diameter of 50 μm. An air Olympus MPLAN (100 ×/0.90NA) objective was used. Raman scattered light was focused onto a multi-mode fibre (50 μm diameter) and monochromator with a 600 mm^{-1}

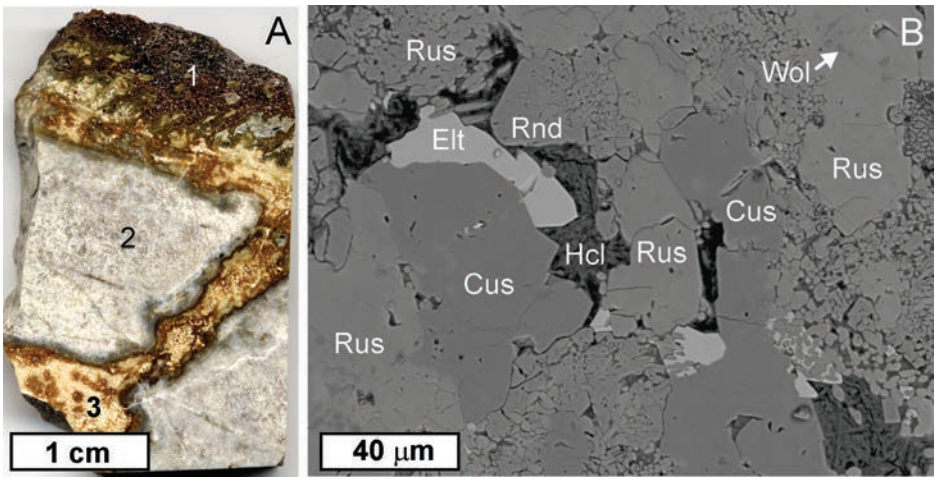

Fig. 1. A: Contact of xenolith with volcanic rock (polished block): 1–volcanic rock, 2–altered xenolith, 3–rusinovite–cuspidine vein. B: Backscattered electron image showing a fragment of rusinovite–cuspidine vein with eltyubyuite. (online version in colour)
Abbreviations: Rus = rusinovite, Cus = cuspidine, Hcl = hydrocalumite, Wol = wollastonite, Elt = eltyubyuite, Rnd = rondorfite.

grating. Some 15–20 scans with integration time of 10–15 s and a resolution of 3 cm^{-1} were collected and averaged. The spectrometer monochromator was calibrated using the Raman scattering line of a silicon plate (520.7 cm^{-1}).

Results

Results of the EMP analysis are listed in Table 2. The Raman spectrum for Al-free eltyubyuite between 100 and 1300 cm^{-1} is shown in Fig 2. The results for single-crystal structure refinement are summarized in Table 1, atomic coordinates and isotropic equivalents (U_{eq}) of anisotropic atom-displacement parameters in Tables 3, anisotropic atomic-displacement parameters in Table 4 and selected interatomic distances in Table 5.

Chemical composition of Al-free eltyubyuite

The chemical composition of eltyubyuite, $Ca_{12.044}(Fe^{3+}_{10.373}Si_{3.473}Ti^{4+}_{0.067}Mn^{2+}_{0.021}Mg_{0.021})_{\sum 13.956}O_{32}Cl_{5.455}$, is rather uniform (Table 1). A simplified crystal chemical formula of eltyubyuite may be written as $Ca_{12}Fe^{3+}_{10.5}Si_{3.5}O_{32}Cl_{5.5}$, which represents a solid solution between the two end-members: 92 % $Ca_{12}Fe^{3+}_{10}Si_4O_{32}Cl_6$ (eltyubyuite), and 8 % $Ca_{12}Fe^{3+}_{14}O_{32}Cl_2$ (theoretical end-member: Fe^{3+}-analogue of chlormayenite). Since eltyubyuite commonly forms a solid solution with wadalite, we expected to find Al at the tetrahedral sites. Instead, the Al_2O_3 content was below the 0.02 wt.% detection limit of the EMP (Table 2).

Table 2. Electron microprobe analysis of the eltyubyuite crystal used for single-crystal study.

wt.%	Mean 7	s.d.	Range
Al_2O_3	n.d.*		
TiO_2	0.29	0.16	0.14–0.51
SiO_2	11.11	0.1	11.08–11.54
Fe_2O_3	44.09	0.7	42.9–45.0
MnO	0.08	0.03	0.03–0.12
CaO	35.95	0.2	35.8–36.3
MgO	0.05	0.06	0.00–0.15
Cl	10.30	0.1	10.07–10.41
$-O = Cl$	2.32		
	99.54		
Ca/***X***	***12.044***		
Fe^{3+}	10.373		
Si	3.473		
Ti^{4+}	0.067		
Mn^{2+}	0.021		
Mg	0.021		
T	***13.956***		
Cl	5.455		

** detection limit $Al_2O_3 = 0.02$ wt%*

$Ca_{12.044}(Fe^{3+}_{10.373}Si_{3.473}Ti^{4+}_{0.067}Mn^{2+}_{0.021}Mg_{0.021})_{\sum 13.956}O_{32}Cl_{5.455}$

Cation charges/anion charges: +69.451/−69.455

Crystal structure of Al-free eltyubyuite

The studied Al-free eltyubyuite is cubic, space group $I\bar{4}3d$, $a = 12.2150$ (2) Å, $V = 1822.55(6)$ Å^3, $Z = 2$, and has the simplified empirical formula $Ca_{12}Fe^{3+}_{10.33}Si_{3.67}O_{32}[Cl_{5.45}]$.

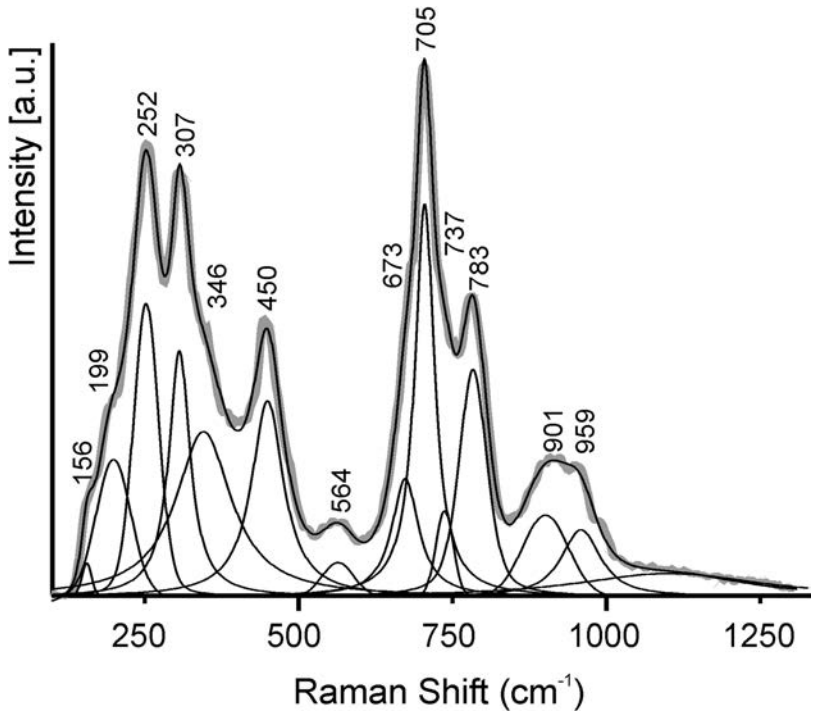

Fig. 2. Raman spectrum of Al-free eltybyuite from Southern Ossetia.

Table 3. Atom coordinates, occupancies, and U_{eq} (Å^2) values for eltyubyuite.

Site	Atom	x	y	z	U_{eq}	Occ.
Ca1	Ca	0.14382(6)	0	0.25	0.0081(3)	1
*T*1	Fe	0.01461(4)	0.01461(4)	0.01461(4)	0.0077(3)	0.848(10)
	Si	0.01461(4)	0.01461(4)	0.01461(4)	0.0077(3)	0.152(10)
*T*2	Fe	0.875	0	0.25	0.0064(3)	0.592(11)
	Si	0.875	0	0.25	0.0064(3)	0.408(11)
O1	O	0.03306(18)	0.44312(18)	0.15402(19)	0.0164(6)	1
O2	O	0.18061(18)	0.18061(18)	0.18061(18)	0.0127(8)	1
W	Cl	0.375	0	0.25	0.0168(6)	0.908(8)

Table 4. Anisotropic displacement parameters U_{ij}.

Site	U_{11}	U_{22}	U_{33}	U_{23}	U_{13}	U_{12}
Ca	0.0091(4)	0.0085(4)	0.0068(4)	0.0007(3)	0.000	0.000
*T*1	0.0077(3)	0.0077(3)	0.0077(3)	−0.0003(2)	−0.0003(2)	−0.0003(2)
*T*2	0.0048(5)	0.0071(4)	0.0071(4)	0.000	0.000	0.000
O1	0.0190(12)	0.0107(12)	0.0196(12)	0.0016(9)	0.0032(9)	−0.0006(9)
O2	0.0127(8)	0.0127(8)	0.0127(8)	0.0036(9)	0.0036(9)	0.0036(9)
W	0.0090(8)	0.0206(7)	0.0206(7)	0.000	0.000	0.000

Table 5. Selected interatomic distances (Å) in eltyubyuite.

Atom 1	Atom 2	Distance
Ca	O1 2x	2.397(2)
	O1 2x	2.555(2)
	O2 2x	2.4057(16)
*T*1	O1 3x	1.872(2)
	O2	1.777(4)
*T*2	O1 4x	1.766(2)

Eltyubyuite, ideally $Ca_{12}Fe^{3+}{}_{10}Si_4O_{32}Cl_6$, is based on a tetrahedral framework $\{T_{14}O_{32}\}$ and is isostructural with mayenite $Ca_{12}Al_{14}O_{32}[O]$ (Büssem & Eitel, 1936). In compounds with mayenite-type structure the framework encloses six structural cages, each occupied by two Ca atoms. The [*W*] site is in a cavity about 5 Å across, which is partially occupied by anions and flanked by Ca atoms (Fig. 3). Depending on the kind of the framework cations (Mg, Al, Si, Fe, Ti) the charge sum of framework plus cage-filling Ca ranges between 2+ (mayenite-group compounds) and 6+ (wadalite-group compounds, Galuskin *et al.*, 2015a). The excess positive charge is balanced by the anions at the [*W*] site. In contrast to mayenite, where all *T* sites are occupied by Al, in eltyubyuite both tetrahedra are Fe^{3+} dominant, with partial occupancy of Si^{4+}.

In the studied Al-free eltyubyuite, the *T*1 site is strongly dominated by Fe^{3+} [site population 0.848(10)] with minor Si^{4+} [0.152(10)]. *T*1 shares three bonds with O1 (*T*1–O1 = 1.872(3) Å), which is the connecting oxygen site of the tetrahedral framework. The fourth apex of the *T*1 tetrahedron points towards the centre of the structural cage and is represented by a bond to O2 (*T*1–O2 = 1.777(3) Å). The *T*1 tetrahedra in eltyubyuite are more distorted compared to those in mayenite and wadalite. The angle O1-*T*1-O2 is 120.32(13)° compared to 118.13(8)° in chlormayenite (Galuskin *et al.*, 2012), 117.04(13)° in fluormayenite (Galuskin *et al.*, 2015b) or 118.00(4)° (Mihajlović *et al.*, 2004) and 118.0(3)° (Tsukimura *et al.*, 1993) in wadalite. The more regular tetrahedron *T*2 contains less Fe^{3+} [site population 0.592(11) Fe and 0.408(11) Si]; it shares four equal bonds with O1 (1.766(2) Å) and has O1-*T*2-O1 angles of 101.02(12)° and 113.86(12)°, respectively.

In the crystal structure of Fe-rich wadalite from Bellerberg volcano (Mihajlović *et al.*, 2004) Si prefers the *T*1 site instead of *T*2, whereas we observe the opposite in eltyubyuite. Neither the wadalite structure of Tsukimura *et al.* (1993) nor the structure of the synthetic wadalite (Feng *et al.*, 1988) shows a clear tendency for Si preference at *T*1 or *T*2. A possible explanation for this observation is the considerable amount of Mg (11 %) at *T*2 in wadalite from Bellerberg (Mihajlović *et al.*, 2004), which leads to a large *T*2 tetrahedron suitable for Al, Fe and Mg but too large for Si. Thus, Si concentrates in the smaller *T*1 tetrahedron. Magnesium is probably restricted to the *T*2 site since oxygen at O2 would easily be underbonded with a divalent cation at *T*1. O1 is linked to *T*1 and *T*2 tetrahedra and binds twice to Ca. Therefore, the bond valence sum at O1 is independent of the individual occupancy of *T*1 and *T*2. This assumption is supported by the synthesis of a wadalite-like compound $Ca_{12}Al_2Mg_4Si_8O_{32}[Cl_6]$ from $CaCl_2$ flux (Gfeller, unpublished data). In this synthetic compound Mg is also located at the *T*2 site, whereas *T*1 is completely occupied by Si.

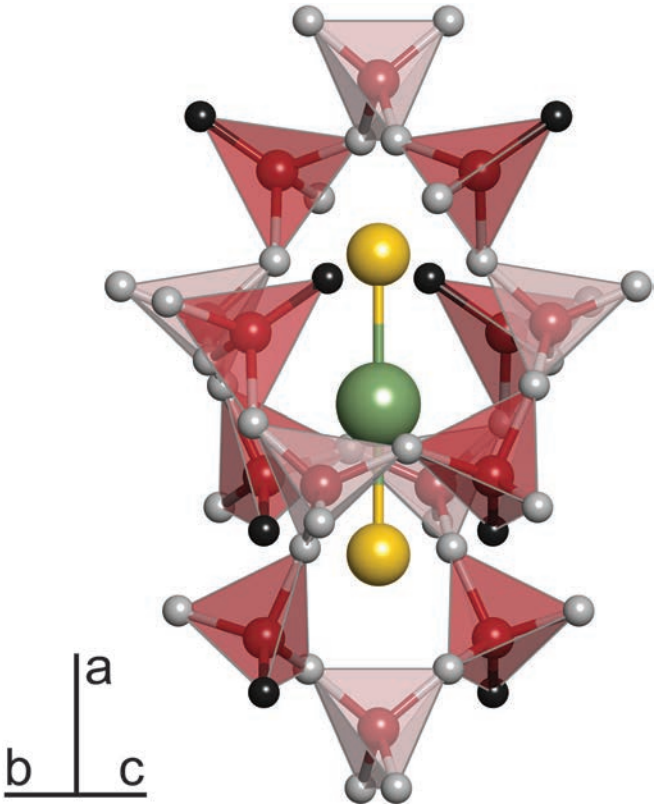

Fig. 3. One of the structural cages in eltyubyuite projected along [011]. The T1 site dominant in Fe (85 % Fe, 15 % Si) is shown as dark red tetrahedra, O1 as grey, O2 as black spheres. T2 (60 % Fe, 40 % Si) is drawn as light-red tetrahedra. In the centre Cl (green sphere) is flanked by two Ca atoms (yellow spheres). The distance between the T2 site on the bottom to the one on the top of drawing corresponds to *a* (12.215 Å). The Ca–Ca distance is 5.648 Å. (online version in colour)

The occupancy of Cl at the [*W*] site of the Al-free eltyubyuite has been refined from single-crystal XRD data and converged to 5.45(5) Cl pfu; the value agrees well with the average EMP analysis (Table 2). The charge-balance of the crystal-chemical formula obtained from structure refinement, $Ca_{12}Fe_{10.33}Si_{3.67}O_{32}Cl_{5.45}$, results in a deficit of 0.2 e^- anionic charge (+69.66/−69.46), which might be explained by neglected minor divalent cations at the *T* sites as well as potential (OH^-) at the [*W*] site. In general, the formula is in good agreement with the empirical formula calculated from EMP data (Tables 1, 2).

Raman spectroscopy

The Raman spectrum of the studied Al-free eltyubyuite (Fig.2) is similar to the spectrum of the holotype eltyubyuite containing 1.45 Al pfu, where the main bands are at about 700, 450 and 300 cm^{-1} (Fig. 4 in Galuskin *et al.*, 2013). The spectrum of the very small holotype eltybyuite sample is of low quality, due to band broadening and contamination by additional bands of larnite and rondorfite (Galuskin *et al.*, 2013). The spectrum of Al-free eltybyuite is characterized by higher spectral resolution. However, the recorded bands have increased half-width due to Fe^{3+} and Si^{4+} disorder at the two tetrahedral sites *T*1 and *T*2. Thus, most bands in the range 300–1300 cm^{-1} are attributed to vibrations in tetrahedra. The bands at 959 and 901 cm^{-1} are related to Si–O stretching vibrations (ν_1 and ν_3) of $(SiO_4)^{4-}$. The group of bands at 783 (ν_3), 705 (ν_1), 450 (ν_4), 307 (ν_2) cm^{-1} are assigned to Fe–O vibration of $(Fe^{3+}O_4)^{5-}$ and are shifted towards lower wavenumbers compared to Al-bearing eltyubyuite (Galuskin *et al.*, 2013). The bands below 300 cm^{-1} (252 and 199 cm^{-1}) are assigned to translational motions of $T(ZO_4)$ and T(Ca) (Tolkacheva *et al.*, 2011; Dulski *et al.*, 2013). The interpretation of a few bands (346, 564, 673, 737 cm^{-1}) is ambiguous. The band at 564 cm^{-1} may be related to both bending $\nu_4(SiO_4)$ and stretching Fe–O–Fe vibrations. The bands at 673 and 737 cm^{-1} are probably related to vibrations of O–Si–O and Si–O–Si, and the band at 346 cm^{-1} is assigned to $\nu_2(SiO_4)$ (Kaindl *et al.*, 2010; Galuskin *et al.*, 2012).

Acknowledgements: F.G. and T.A. acknowledge support by the Swiss National Science Foundation project ''Crystal Chemistry of Minerals'' 200020_134617, D.Ś. thanks for the support of the scholarship programme DoktoRIS.

References

Bowers, M., Collon, P., Kashiv, Y., Bauder, W., Chamberlin, K., Lu, W., Robertson, D., Schmitt, C. (2013): First experimental results of the ^{33}S (α, p)^{36}Cl cross section for production in the early solar system. *Nucl. Instrum. Methods B: Beam Interact. Mater. Atoms*, **294**, 491–495.

Bricker, G.E. & Caffee, M.W. (2013): Incorporation of ^{36}Cl into Calcium-Aluminum-Rich Inclusions in the Solar Wind Implantation Model. *Adv. Astr.*, Article ID 487606, 4 pages

Büssem, W. & Eitel, A. (1936): Die Struktur des Pentacalciumtrialuminats. *Z. Kristallogr.*, **95**, 175–188.

Cebocli, A., Garcin, P., Geissbühler, U. (2007): *U.S. Patent No. 7,226,071*. Washington, DC: U.S. Patent and Trademark Office.

Dulski, M., Bulou, A., Marzec, K.M., Galuskin, E.V., Wrzalik, R. (2013): Structural characterization of rondorfite, calcium silica chlorine mineral containing magnesium in tetrahedral position $[MgO_4]^{6-}$, with the aid of the vibrational spectroscopy and fluorescence. *Spectrochim. Acta A Mol. Biomol. Spectrosc.*, **15**, 382–388.

Feng, Q.L., Glasser, F.P., Howie, R.A., Lachowski, E.E. (1988): Chlorosilicate with the $12CaO.7Al_2O_3$ structure and its relationship to garnet. *Acta Crystallogr. C*, **44**, 589–592.

Fujita, S., Suzuki, K., Ohkawa, M., Shibasaki, Y., Mori, T. (2001): Reaction of hydrogrossular with hydrogen chloride gas at high temperature. *Chem. Mater.*, **13**, 2523–2527.

Fujita, S., Suzuki, K., Mori, T., Shibasaki, Y. (2003): A new technique to remove hydrogen chloride gas at high temperature using hydrogrossular. *Ind. Eng. Chem.*, **42**, 1023–1027.

Galuskin, E.V., Galuskina, I.O., Stadnicka, K., Armbruster, T., Kozanecki, M. (2007): The crystal structure of Si-deficient, OH-substituted, boron-bearing vesuvianite from the Wiluy River, Sakha-Yakutia, Russia. *Can. Mineral.*, **45**, 239–248.

Galuskin, E.V., Kusz, J., Armbruster, T., Bailau, R., Galuskina, I.O., Ternes, B., Murashko, M. (2012): A reinvestigation of mayenite from the type locality, the Ettringer Bellerberg volcano near Mayen, Eifel district, Germany. *Mineral. Mag.*, **76**, 707–716.

Galuskin, E.V., Galuskina, I.O., Bailau, R., Prusik, K., Gazeev, V.M., Zadov, A.E., Pertsev, N.N., Jeżak, L., Gurbanov, A.G., Dubrovinsky, L. (2013): Eltyubyuite, $Ca_{12}Fe^{3+}{}_{10}$ Si $_4O_{32}Cl_6$ - the Fe^{3+} analogue of wadalite: a new mineral from the Northern Caucasus, Kabardino-Balkaria, Russia. *Eur. J. Mineral.*, **25**, 221–229.

Galuskin, E.V., Gfeller, F., Galuskina, I.O., Armbruster, T., Bailau, R., Sharygin, V.V. (2015a): Mayenite supergroup, part I: recommended nomenclature. *Eur. J. Mineral.*, **27**, DOI: 10.1127/ejm/2015/0027-2418

Galuskin, E.V., Gfeller, F., Armbruster, T., Galuskina, I.O., Vapnik, Ye., Dulski, M., Murashko, M., Dzierżanowski, P., Sharygin, V.V., Krivovichev, S.V., Wirth, R. (2015b): Mayenite supergroup, part III: fluormayenite, $Ca_{12}Al_{14}O_{32}$ [$\square_4F_2$], and fluorkyuygenite, $Ca_{12}Al_{14}O_{32}[(H_2O)_4F_2]$, two new minerals of from pyrometamorphic rock of Hatrurim Complex South Levant. *Eur. J. Mineral.*, **27** DOI: 10.1127/ejm/2015/0027-2420

Gazeev, V.M., Gurbanova, O.A., Zadov, A.E., Gurbanov, A.G., Leksin, A.B. (2012): Mineralogy of skarned carbonate xenoliths from Shadil-Khokh volcano (Kelski volcanic area of the Great Caucasian Range). *Vestnik Vladikavkazskogo Nauchnogo Centra*, **2**, 18–27. (in Russian)

Hršelová, P., Cempírek, J., Houzar, S., Sejkora, J. (2013): S, F, Cl-rich Mineral Assemblages from burned spoil heaps in the Rosice-Oslavany Coalfield, Czech Republic. *Can. Mineral.*, **51**(**1**), 171–188.

Ishii, H.A., Krot, A.N., Bradley, J.P., Keil, K., Nagashima, K., Teslich, N., Jacobsen, B., Yin, Q.Z. (2010): Discovery, mineral paragenesis, and origin of wadalite in a meteorite. *Am. Mineral.*, **95**(**4**), 440–448.

Ito, S. & Webster, S. (2007): U.S. Patent Application *11/950,433*.

Ito, K., Watanabe, S., Miyakawa, N., Kuroiwa, Y., Ito, S. (2012): U.S. Patent Application *13/404,870*.

Kaindl, R., Többens, D.M., Kahlenberg, V. (2010): DFT-aided interpretation of the Raman spectra of the polymorphic forms of $Y_2Si_2O_7$. *J. Raman Spectrosc.*, **42**, 78–85.

Kanazawa, Y., Aoki, M., Takeda, H. (1997): Wadalite, rustumite, and spurrite from La Negra mine, Queretaro, Mexico. *Bull. Geol. Sur. Jpn.*, **48**, 413–420.

Lee, D.K., Kogel, L., Ebbinghaus, S.G., Valov, I., Wiemhoefer, H.D., Lerch, M., Janek, J. (2009): Defect chemistry of the cage compound, $Ca_{12}Al_{14}O_{33}-\delta$—understanding the route from a solid electrolyte to a semiconductor and electride. *Phys. Chem. Chem. Phys.*, **11**, 3105–3114.

Leturcq, G., Grandjean, A., Rigaud, D., Perouty, P., Charlot, M. (2005): Immobilization of fission products arising from pyrometallurgical reprocessing in chloride media. *J. Nucl. Mater.*, **347**, 1–11.

Matzel, J.E.P., Jacobsen, B., Hutcheon, I.D., Krot, A.N., Nagashima, K., Yin, Q., Ramon, E., Weber, P.K., Wasserburg, G.J. (2010): Distribution and origin of ^{36}Cl in Allende CAIs. *Lunar and Planetary Institute Science Conference Abstracts*, **41**, 2631

Mihajlović, T., Lengauer, C.L., Ntaflos, T., Kolitsch, U., Tillmanns, E. (2004): Two new minerals, rondorfite, $Ca_8Mg[SiO_4]_4Cl_2$, and almarudite, $K(\square, Na)_2(Mn,Fe,Mg)_2(Be,Al)_3[Si_{12}O_{30}]$, and a study of iron-rich wadalite, $Ca_{12}[(Al_8Si_4Fe_2)O_{32}]Cl_6$, from the Bellerberg (Bellberg) volcano, Eifel. *N. Jb. Mineral. Abh.*, **179**, 265–294.

Palacios, L., De La Torre, A.G., Bruque, S., García-Muñoz, J.L., García-Granda, S., Sheptyakov, D., Aranda, M.A. (2007): Crystal structures and in-situ formation study of mayenite electrides. *Inorg. Chem.*, **46**, 4167–4176.

Palacios, L., Cabeza, A., Bruque, S., García-Granda, S., Aranda, M.A. (2008): Structure and electrons in mayenite electrides. *Inorg. Chem.*, **47**, 2661–2667.

Park, H.S., Kim, I.T., Cho, Y.Z., Eun, H.C., Lee, H.S. (2008): Stabilization/Solidification of Radioactive Salt Waste by Using $\square$ SiO_2- y Al_2O_3- z P_2O_5 (SAP) Material at Molten Salt State. *Environ. Sci. Technol.*, **42**, 9357–9362.

Sakakura, T., Tanaka, K., Takenaka, Y., Matsuishi, S., Hosono, H., Kishimoto, S. (2011): Determination of the local structure of a cage with an oxygen ion in $Ca_{12}Al_{14}O_{33}$. *Acta Crystallogr.*, **B67**, 193–204.

Sharygin, V.V. (2010): Mineralogy of Ca-rich metacarbonate rocks from burned dumps of the Donetsk Coal Basin. *in* Proceedings of ''ICCFR2-Second International Conference on Coal Fire Research'', 162–170.

Sheldrick, G.M. (2008): A short history of SHELX. *Acta Crystallogr.*, **A64**, 112–122.

Tolkacheva, A.S., Shkerin, S.N., Plaksin, S.V., Vovkotrub, E.G., Bulanin, K.M., Kochedykov, V.A., Ordinartsev, D.P., Gyrdasova, O.I., Molchanova, N.G. (2011): Synthesis of dense ceramics of single-phase mayenite $(Ca_{12}Al_{14}O_{32})O$. *Russ. J. Appl. Chem.*, **84**, 907–911.

Tsukimura, K., Kanazawa, Y., Aoki, M., Bunno, M. (1993): Structure of wadalite $Ca_6Al_5Si_2O_{16}Cl_3$. *Acta Crystall.*, **C49**, 205–207.

Watanabe, S., Miyakawa, N., Kuroiwa, Y., Ito, K., Ito, S., Maeda, K. (2012): U.S. Patent Application *13/403,325*.

Received 4 August 2014
Modified version received 10 October 2014
Accepted 11 October 2014